

Tamoxifen-like metallocifens target thioredoxin system determining mitochondrial impairment leading to apoptosis in Jurkat cells

Received 00th January 20xx,
Accepted 00th January 20xx

DOI: 10.1039/x0xx00000x

www.rsc.org/

Valeria Scalcon,^{a*} Michèle Salmain,^{b*} Alessandra Folda,^a Siden Top,^b Pascal Pigeon,^{b,c} Hui Zhi Shirley Lee,^{b,c} Gérard Jaouen,^{b,c} Alberto Bindoli,^d Anne Vessières,^{b**} and Maria Pia Rigobello^{a**}

Abstract

Tamoxifen-like metallocifens (TLMs) of the group-8 metals (Fe, Ru, Os) show strong anti-proliferative activity on cancer cell lines resistant to apoptosis, owing to their unique redox properties. On the other hand, the thioredoxin system, which is involved in cellular redox balance, is often overexpressed in cancer cells, especially in tumour types resistant to standard chemotherapies. Therefore, we investigated the effect of these three TLMs on the thioredoxin system and evaluated the input of the metallocene unit by comparison with structurally related organic tamoxifens. *In vitro*, all three TLMs became strong inhibitors of the cytosolic (TrxR1) and mitochondrial (TrxR2) isoforms of thioredoxin reductase **and** after enzymatic oxidation with HRP/H₂O₂ while none of the organic analogues was effective. In Jurkat cells, TLMs inhibited mainly TrxR2, resulting in accumulation of oxidized thioredoxin 2 and cell redox imbalance. Overproduction of ROS ensued in a strong decrease of mitochondrial membrane potential, translocation of cytochrome c to the cytosol and activation of caspase 3, thus leading to apoptosis. None of these events occurred with organic tamoxifens. The mitochondrial fraction of cells exposed to TLMs contained a high amount of the corresponding metal as quantified by ICP-OES. The lipophilic and cationic character associated with the singular redox properties of the TLMs could explain why they alter the mitochondrial function. These results provide new insights into the mechanism of action of tamoxifen-like metallocifens, underlying their prodrug behaviour and the pivotal role played by the metallocenic entity in their cytotoxic activity associated with induction of apoptosis.

Significance to Metallomics

Biological effects of tamoxifen-like metallocifens (TLMs) of iron, ruthenium and osmium on Jurkat cells were compared to those of the corresponding organic tamoxifens. All three TLMs behaved as strong inhibitors of mitochondrial thioredoxin reductase both *in vitro* and in Jurkat cells, induced mitochondrial membrane depolarization and eventually cell apoptosis. The organic molecules were inactive in this set of experiments thus underlying the role of the metals. These effects are associated to the unique redox properties of the metallocene units and charge-driven accumulation of TLMs in mitochondria. Among the three compounds, the ferrocenyl TLM appears as the most active.

Introduction

Breast cancer remains the most common malignancy in women, and despite the efforts that have been put on its early detection half a million people died from this disease in 2012.¹ Early breast cancer is now considered potentially curable and tamoxifen administration is the standard endocrine therapy of hormone receptor positive breast cancer. This is not the case for metastatic breast cancers, which are

heterogeneous, often resistant to apoptosis and consequently difficult to cure. Thus, the search for new drugs, with mechanisms of action different from those already in use are urgently needed. Some of us introduced sometime ago ferrocenyl analogues of **OH-tamoxifen (OH-Tam[2]**, chart 1), an active metabolite of tamoxifen.^{2,3} Not only these compounds kept an anti-oestrogenic effect on hormone-dependent breast cancer cells but they also displayed a high cytotoxicity on the triple negative breast cell line MDA-MB-231 (IC₅₀ = 0.5 μM for **Fc-OH-Tam**)³ as well as on a panel of cells resistant to apoptosis (glioma, melanoma).^{4,5} In addition, **Fc-OH-Tam** significantly inhibited *in vivo* growth of MDA-MB-231 xenografted tumours in mice when formulated in lipid nanocapsules (LNC).⁴ Regarding the mechanism of action of this complex, we found that

a) Dipartimento di Scienze Biomediche, Università di Padova, Via Ugo Bassi 58/b, 35131 Padova, Italy.

b) Sorbonne Universités, UPMC Univ Paris 06, CNRS, Institut Parisien de Chimie Moléculaire (IPCM), F-75005 Paris, France

c) Chimie ParisTech, 11 rue Pierre et Marie Curie, F-75005 Paris, France

d) Istituto di Neuroscienze (CNR) Sezione di Padova, c/o Dipartimento di Scienze Biomediche, Via Ugo Bassi 58/b, 35131 Padova, Italy.

* Valeria Scalcon and Michèle Salmain contributed equally to the work

** Anne Vessières and Maria Pia Rigobello: co-corresponding authors

Electronic Supplementary Information (ESI) available: [details of any supplementary information available should be included here]. See DOI: 10.1039/x0xx00000x

Fc-OH-Tam induced strong senescence in MDA-MB-231 as compared to low apoptosis.⁶ These remarkable properties have been linked to the presence of the [Fc-ene-phenol] motif that is selectively activated in cancer cells, therefore revealing their redox environment.⁷ As such **Fc-OH-Tam** acts as a prodrug whose cytotoxicity is associated to its oxidation to a highly electrophilic quinone methide.⁷ More recently we found that the quinone methide of **Fc-OH-Tam** was able to strongly inhibit the enzyme thioredoxin reductase (TrxR) *in vitro*.⁸ TrxR belongs to the thioredoxin system that is responsible for thiol redox homeostasis together with the glutathione system. It is present as cytosolic (TrxR1) and mitochondrial (TrxR2) isoforms, both displaying a selenocysteine residue at their C-terminal active site, which acts as a major target of electrophiles as well as many metal complexes.⁹⁻¹² TrxR is often overexpressed in cancer cells and its inhibition may lead to cell apoptosis.^{13,14} **Fc-OH-Tam** inhibits TrxR in Jurkat cells, indicating that its conversion to quinone methide occurs *in cellulo* via endogenous oxidizing systems. Recent studies on the tamoxifen-like complex of osmium (**Oc-OH-Tam**, chart 1) showed that *in vitro* inhibition of TrxR only occurred after its enzymatic oxidation by the HRP/H₂O₂ mixture. Although less cytotoxic than **Fc-OH-Tam** on MDA-MB-231 cell line (IC₅₀ = 2.7 μM)¹⁵, **Oc-OH-Tam** proved to be an effective inhibitor of TrxR in Jurkat cells inducing mitochondrial dysfunction and cell death.¹⁶

In order to get a better insight into the mechanism of action of tamoxifen-like metallocens (TLMs) and to evaluate the role played by the metalocenic unit we report here the comparison of some biological effects of TLMs of iron, ruthenium and osmium with those of their organic tamoxifen analogues (Chart 1). Experiments included *in vitro* studies on purified cytosolic and mitochondrial isoforms of TrxR (TrxR1 and TrxR2) followed by studies on mitochondrial functionality in Jurkat cells. In particular, the redox state of mitochondrial Trx, ROS level and mitochondrial membrane potential (MMP) were measured. In addition, the intracellular distribution of metals was determined by ICP-OES measurements. On the whole, only TLMs and not their organic analogues were able to initiate cell apoptosis via mitochondria-mediated pathway.

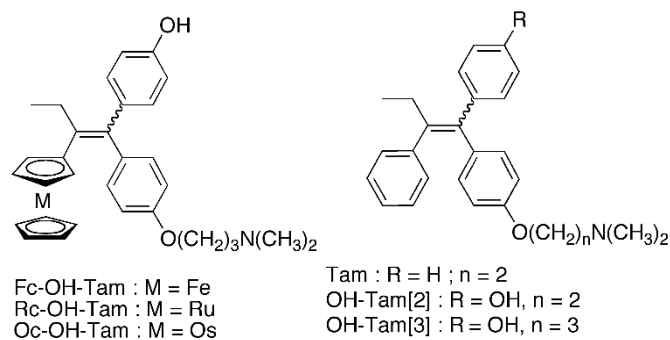


Chart 1 : Formulae of the compounds under study

Experimental

Materials

Stock solutions of the compounds (1×10^{-2} M) were prepared in DMSO and were stable for at least two months if kept at 4 °C. Horseradish peroxidase (HRP), yeast glutathione reductase, **Tam**, and **OH-Tam[2]**, iodoacetamide (IAM), iodoacetic acid (IAA), DTNB and metal standards were purchased from Sigma Aldrich (Saint Louis, MO, USA). BIAM, TMRM, DHR and MitoSOX were purchased from Invitrogen (Thermo Fisher Scientific, Waltham, MA, USA). Primary antibodies utilized: Trx2 monoclonal antibody (H75) and caspase-3 polyclonal antibody clone H-277 (Santa Cruz Biotechnology, Santa Cruz, CA, USA); cytochrome c clone 7H8.C12 (BioSource International, Inc., Camarillo, CA, USA); anti-cytochrome c oxidase subunit 4 monoclonal antibody 1D6 (Thermo Fisher Scientific, Waltham, MA, USA).

Enzymatic oxidation of the compounds by the HRP/H₂O₂ mixture

Enzymatic oxidation of the compounds (25 - 50 μM) by HRP (46 nM) and H₂O₂ (200 μM) was performed at pH 8.1 in buffer (0.2 M Tris-HCl, 1 mM EDTA) containing 10% DMSO. HRP (40 μL of 1.14 μM solution) and H₂O₂ (20 μL of 10 mM solution) were pre-incubated for 5 min then added to the solution of the compounds (940 μL). The solution was immediately transferred to a cuvette and the UV-Visible spectrum was recorded between 250 and 600 nm every 30 s on a Cary 50 spectrometer (Varian, Palo Alto, CA, USA). Rate constants k_{obs} were calculated, with Kaleidagraph software, by fitting OD_{324nm} (**Oc-OH-Tam**), OD_{413nm} (**Fc-OH-Tam**), OD_{418nm} (**Rc-OH-Tam**) and OD_{279nm} (**OH-Tam[3]**) versus time data according to the first order law equation : $OD = C_0 + C_1 \times \exp(-k_{\text{obs}} \times t)$.

Enzymatic activity estimation of isolated TrxR1 and TrxR2

Highly purified cytosolic (TrxR1) and mitochondrial (TrxR2) thioredoxin reductase were prepared from rat liver according to

Luthman and Holmgren¹⁷ and to Rigobello and Bindoli,¹⁸ respectively. The protein content of purified enzyme preparations was measured according to Lowry *et al.*¹⁹ Thioredoxin reductase activity was determined by estimating the DTNB-reducing property of the enzymes in the presence of NADPH. Aliquots of highly purified TrxR1 or TrxR2 in 0.2 M Tris-HCl buffer (pH 8.1), 1 mM EDTA and 0.25 mM NADPH were pre-incubated for 5 min with the various compounds. Afterward, the reaction was initiated with 1 mM DTNB and monitored spectrophotometrically at 412 nm for about 10 min. For the oxidized metallocifens derivatives formation, freshly prepared compounds at increasing concentrations were incubated for 15 min in 0.2 M Tris-HCl buffer (pH 8.1) containing 1 mM EDTA, with 0.1 mM H₂O₂ and 22 nM HRP. Then, TrxR aliquot and 0.25 mM NADPH were added and incubated for 5 min. Finally, the reaction was initiated with 1 mM DTNB and monitored spectrophotometrically at 412 nm for about 10 min.

BIAM assay

First, TLMs and organic tamoxifen were treated with the mixture of 22 nM HRP/0.1 mM H₂O₂ for 15 min as reported in the previous paragraph. Then, 1 μ M TrxR pre-reduced in the presence 60 μ M NADPH, was incubated with 2 μ M of the obtained derivatives for 30 min at room temperature, in 50 mM Tris-HCl buffer (pH 7.4) containing 200 μ M NADPH and 1 mM EDTA. After incubation, 8 μ L of the reaction mixture was added to 8 μ L of 100 μ M biotinylated iodoacetamide (BIAM) in 0.1 M Tris-HCl at pH 8.5 or in 0.1 M Hepes-Tris pH 6.0.²⁰ Samples were incubated at room temperature for an additional 30 min to allow BIAM alkylation of free -SH/SeH groups of the enzyme. Then, BIAM-modified enzyme was subjected to sodium dodecyl sulphate-polyacrylamide gel electrophoresis (SDS-PAGE) on a 10% gel, and transferred to a nitrocellulose membrane. BIAM labelled enzyme was detected with horseradish peroxidase-conjugated streptavidin and enhanced chemiluminescence detection.

Determination of total thioredoxin reductase activity in Jurkat cell lysates

The human leukemic lymphoblastoid Jurkat cells were cultured in RPMI 1640 medium supplemented with 2 mM L-glutamine, 10% FBS and 1% penicillin/streptomycin (Invitrogen), at 37 °C in a humidified atmosphere of 95% air and 5% CO₂. Cells (2 x 10⁶) were incubated with 15 μ M compounds for 18 h, then harvested and washed with PBS. Each sample was lysed with a modified RIPA buffer: 150 mM NaCl, 50 mM Tris-HCl, 1 mM EDTA, 1% Triton X-100, 0.1% SDS, 0.5%

DOC, 1 mM NaF and an antiprotease cocktail ("Complete" Roche, Mannheim, Germany) containing 0.1 mM PMSF. After 40 min at 4 °C, lysates were centrifuged at 12000g for 6 min. The supernatants were tested for total TrxR activity. Therefore, aliquots of lysates (12 μ g proteins) were incubated for 40 min in a final volume of 50 μ L in 100 mM Hepes-Tris buffer (pH 7.6), in the presence of 15 mM EDTA, 1.5 mM NADPH, 0.20 mM insulin, and 100 μ M Trx from *E. coli*. The reaction was stopped by the addition of 0.2 mL of 1 mM DTNB in 0.2 M Tris-HCl buffer (pH 8.1) containing 1 mM EDTA and 7.2 M guanidine, and samples O.D. was estimated at 412 nm²¹ on a plate reader (Tecan Infinite® M200 PRO, Männedorf, CH).

Preparation of cytosol and mitochondria enriched fractions and evaluation of thioredoxin reductase activity

To obtain cytosolic and mitochondrial fractions, Jurkat cells (3 x 10⁷) were grown in 75 cm² flasks and then treated with the various compounds (30 μ M) for 18 h. After incubation, cells were processed to obtain mitochondria and cytosol enriched fractions essentially following the protocol of Clayton and Shadel.²² Briefly, cells were collected, washed with PBS and subjected to hypo-osmotic treatment with 2 mL of 10 mM NaCl, 1.5 mM MgCl₂ and 10 mM Tris-HCl (pH 7.5) for 5 min and gently homogenized using a Dounce tissue grinder. After this treatment, 1.4 mL of 525 mM mannitol, 175 mM sucrose, 12.5 mM Tris-HCl (pH 7.5) with 2.5 mM EDTA (pH 7.5) were rapidly added. Then, the homogenate was diluted to a final volume of 5 mL with 210 mM mannitol, 70 mM sucrose, 5 mM Tris-HCl (pH 7.5) buffer, 1 mM EDTA (pH 7.5) and subjected to differential centrifugation. The first step was carried out at 1300g for 5 min at 4 °C to discard nuclei and non-disrupted cells. The mitochondrial enriched-fraction was pulled down from the supernatant at 15800g for 15 min at 4 °C and washed twice. The crude soluble supernatant obtained from the mitochondrial isolation step, was further centrifuged at 105000g for 15 min in order to obtain the cytosolic fraction. Afterward, mitochondrial samples were lysed using a modified RIPA buffer, as reported in the previous paragraph, and subjected to protein determination with the Lowry assay.¹⁹ In addition, the presence of cytochrome oxidase as a mitochondrial marker was assessed by Western blot analysis, using an anti-cytochrome c oxidase subunit 4 monoclonal antibody 1D6. Both cytosolic and mitochondrial fractions (50 μ g of proteins) were then tested for thioredoxin reductases activity, in a buffer containing 0.2 M NaKPi, 5 mM EDTA (pH 7.4) with 20 mM DTNB. After 2 min, 0.25 mM NADPH was added and the reaction was followed at 412 nm at

25 °C using a Lambda 2 spectrophotometer (PerkinElmer, Waltham, MA, USA).

Redox Western Blot Analysis of Trx2

The redox state of Trx was detected using a modified Western blot analysis.^{23,24} Briefly, after treatment with the compounds (15 µM) for 18 h, Jurkat cells (2×10^6) were washed with PBS and lysed in 100 µL of urea lysis buffer (100 mM Tris-HCl, pH 8.3, containing 1 mM EDTA, 8 M urea, and 10 mM IAM) in order to alkylate free thiols. Incubation was carried out at 37 °C for 20 min. Then, cell lysates were spun down and precipitated by ice-cold acetone-1 M HCl (98:2). The pellets were washed twice with ice-cold acetone-1 M HCl-H₂O (98:2:10) and re-suspended in 60 µL of urea lysis buffer including 3.5 mM DTT and incubated for 30 min at 37 °C to reduce the disulfide bonds. Afterward, 3 µL of 600 mM IAM (final concentration 30 mM) were added to the samples, followed by incubation for 30 min at 37 °C. Protein concentration was determined by the Lowry assay.¹⁹ Proteins were separated by urea-PAGE (7% acrylamide/bis(acrylamide) in 7 M urea) and blotted on a nitrocellulose membrane using Trans-Blot® Turbo™ System (Bio-Rad Laboratories, Hercules, CA, USA). Membranes were probed with the primary antibody for Trx2 (H75).

Flow cytometric analysis of the mitochondrial membrane potential and superoxide production in Jurkat cells

Drug-influenced cell mitochondrial membrane potential was analyzed by flow cytometry with the fluorescent probe tetramethyl rhodamine methyl ester (TMRM). Jurkat cells (2×10^6) were treated for 18 h with the compounds (15 µM) and then harvested and re-suspended in PBS/10 mM glucose/25 nM TMRM (final concentration) for 15 min at 37 °C in the dark. Induced changes of membrane potential were estimated with a FACSCanto™ II flow cytometer (Becton-Dickinson, CA, USA) using an argon laser at 585 nm. Cell cultured and treated in the same conditions described above, were also probed for mitochondrial superoxide production utilizing the fluorescent probe MitoSOX™ Red. After treatment with the complexes, Jurkat cells (5×10^5) were incubated with 1 µM MitoSOX™ in PBS/10mM glucose for 25 min in the dark, then diluted (1:4) and analyzed on FACSCanto™ using an argon laser at 585 nm.

Determination of short-term cellular ROS production in Jurkat cells

Jurkat cells (4×10^5 per well) were seeded in a 96 well plate in PBS/10 mM glucose and then incubated for 1 h with 15 µM dihydrorhodamine 123 (DHR) at 37 °C, 5% CO₂. Afterwards, the medium was removed and each well was added with 100 µM PBS/10 mM glucose supplemented with 10 µM TLMs or organic tamoxifen

derivatives. Finally, ROS production was estimated monitoring the fluorescence increase of the probe ($\lambda_{Ex}= 500$ nm, $\lambda_{Em}= 536$ nm), using a Tecan Infinite® M200 PRO plate reader.

Estimation of cytochrome c release and caspase-3 activation

Cytochrome c release and caspase-3 activation were detected by Western blot technique. After 18 h of incubation in presence of 15 µM of the compounds, Jurkat cells (2×10^6) were harvested, washed with PBS, and treated with a hypotonic lysis buffer (20 mM HEPES-Tris buffer (pH 7.5), 10 mM KCl, 1.5 mM MgCl₂, 1 mM EDTA and 1 mM EGTA) added with an antiprotease cocktail (Complete, Roche, Mannheim, DE) for 15 min. Then, the suspension was centrifuged at 12500g for 10 min at 4 °C. The supernatant added with 0.5 mM EGTA and 2.5 mM PMSF, was centrifuged for 30 min at 10000g at 4 °C to obtain the cytosolic fraction. The pellet obtained from the first centrifugation was lysed in the previously reported modified RIPA buffer. Aliquots of 10 µg protein of the supernatants or of the pellets were subjected to SDS-PAGE (15%) followed by Western blot using a cytochrome c monoclonal antibody clone 7H8.C12 and a caspase-3 polyclonal antibody clone H-277. A peroxidase-conjugated secondary antibody and chemiluminescence were used to detect the immunoreactive bands.

Metal quantification in Jurkat cell compartments by ICP-OES

Jurkat cells (3×10^7 cells) incubated for 18 h in the presence of the compounds (30 µM) were subjected to cell fractionation as reported in a previous paragraph. For ICP-OES experiments, mitochondria and crude nuclei fractions were dissolved in 0.54 mL HCl (37%, Fluka for trace analysis) and digested at 60 °C in an ultrasound bath for 1 h. Then the samples volume was brought to 10 mL by addition of water ([HCl] in the sample = 2%). The cytosol samples were adjusted to 2% HCl by addition of proper volumes of 37% HCl and water (final volume = 10 mL). All the solutions were filtered on a 0.45 µm syringe filter. Quantification of iron, ruthenium and osmium was performed at 238.204, 267.876 and 225.585 nm, respectively using an Agilent 5100 instrument (Santa Clara, CA, USA). Metal standards (Fe, Ru and Os) were prepared from 1000 ppm stock solutions. The concentrations used for calibration were in all cases 0, 7.8, 15.6, 31.2, 62.5, 125, 250 and 500 ppb. Measurements were done in triplicate in two or three sets of independent experiments. HCl was used instead of HNO₃ as the latter leads to the formation of the highly toxic and volatile OsO₄. ICP-OES experiments were performed on the ALIPP6 platform at University Pierre et Marie Curie, Paris on a Agilent 5100 instrument.

Statistical analysis

All the experiments reported, if not indicated, are the mean with respective SD of, at least, 4 experiments. The statistical analysis of variance (ANOVA) was performed using Tukey test with INSTAT 3.3 (GraphPad) software.

Results

Synthesis

TLMs of the group-8 metals **Fc-OH-Tam**, **Rc-OH-Tam** and **Oc-OH-Tam** (Chart 1) used in this study were prepared following previously reported protocols and are stable for months in the solid state.^{3,15,25} TLMs are obtained as a mixture of *Z* and *E* stereoisomers. We previously found that these stereoisomers rapidly isomerize in protic medium. Thus the experiments reported herein were performed with mixtures of (*Z*+*E*) isomers of the 3 complexes. The biochemical behaviour of the TLMs was systematically compared to that of 3 analogous organic tamoxifens, namely Tam, its active metabolite **OH-Tam[2]** and **OH-Tam[3]**, the organic analogue including the same dimethylamino-terminated side chain as in the three TLMs which was prepared according to the literature.²⁶

Identification of the products of enzymatic oxidation by HRP/H₂O₂ mixture

Enzymatic oxidation of TLMs and their organic counterparts by the HRP/H₂O₂ mixture was monitored by UV-visible spectrometry. For **Fc-OH-Tam**, progressive appearance of an intense band at 402 nm was observed which was readily assigned to the quinone methide by comparison with the authentic product obtained by chemical oxidation with Ag₂O (Fig. S1-A).^{7,27} This conversion corresponds to a 2-electrons, 2-protons abstraction pathway. The same behaviour was found for **Rc-OH-Tam** for which a band at 418 nm was observed upon oxidation with HRP/H₂O₂ (Fig. S1-B). In contrast, enzymatic oxidation of **OH-Tam[3]** led to the rapid disappearance of its characteristic band at 279 nm but no new peak appeared on the spectra (Fig. S1-C). Thus, treatment of **OH-Tam[3]** by HRP/H₂O₂ did not afford the quinone methide which is characterized by an intense band around 400 nm.²⁸ Previous literature data demonstrated that

HRP oxidation of **OH-Tam[2]** rather affords unstable radical species that tend to polymerize.²⁹ We previously found that enzymatic oxidation of **Oc-OH-Tam** did not afford a quinone methide as did chemical oxidation with Ag₂O but rather led to a quinone methide carbocation characterized by a band at 331 nm resulting from a two-electrons, 1-proton abstraction pathway.¹⁶ This unusual behaviour was assumed to originate from the high stability of carbenium ions derived from osmocene derivatives.^{30,31} Table 1 summarizes the oxidation pathway of the compounds under study and the rate constants of oxidation upon treatment with HRP/H₂O₂. As it appears, oxidation of all the compounds proceeded swiftly, with a slightly faster rate observed for ferrocifen than for ruthenocifen and osmocifen.

Table 1. Summary of enzymatic oxidation experiments

Compound	Oxidation pathway	λ_{\max} (nm)	Nature of oxidation product	Rate constant of oxidation (min ⁻¹)
Fc-OH-Tam	-2e ⁻ /-2H ^{a)}	402	QM	0.521 ± 0.022 ^{d)}
Rc-OH-Tam	-2e ⁻ /-2H	418	QM	0.319 ± 0.008 ^{d)}
Oc-OH-Tam	-2e ⁻ /-1H ^{b)}	331	QM ⁺	0.305 ± 0.002 ^{d)}
OH-Tam[3]	-1e ⁻ /-1H ^{c)}	none	n.d.	0.471 ± 0.02 ^{e)}

a) data from ref ⁸; b) data from ref ¹⁶; c) data from ref ²⁹; d) rate constant of QM or QM⁺ formation; e) rate constant of substrate disappearance

In vitro inhibition studies on TrxR1 and TrxR2

The possible inhibitory activity of the three TLMs and the three organic analogues was first investigated on TrxR1 and TrxR2 purified from rat liver. Experimentally, mixtures of pre-reduced TrxR1 or TrxR2 and various concentrations of each compound were incubated for 5 min before their enzymatic activity was measured. Table 2 gathers the IC₅₀ values deduced from these experiments.

Table 2. *In vitro* inhibitory effect of tamoxifen-like metallocifens and organic tamoxifen derivatives on cytosolic (TrxR1) and mitochondrial (TrxR2) thioredoxin reductase

Compound	IC ₅₀ (μM) ^{a)}		IC ₅₀ after treatment with H ₂ O ₂ /HRP ^{b)} (μM)	
	TrxR1	TrxR2	TrxR1	TrxR2
Fc-OH-Tam	15 ± 2 ^{c)}	32 ± 3	0.06 ± 0.02	10.9 ± 1.2
Rc-OH-Tam	62 ± 2	> 100	0.42 ± 0.08	4.6 ± 0.1
Oc-OH-Tam	40 ± 3.5	23 ± 3	1.2 ± 0.1 ^{d)}	3.9 ± 0.1
Tam	> 100	> 100	> 10	> 10
OH-Tam[2]	> 100	> 100	8.7 ± 1.1	> 10
OH-Tam[3]	> 100	> 100	8.1 ± 0.8	> 10

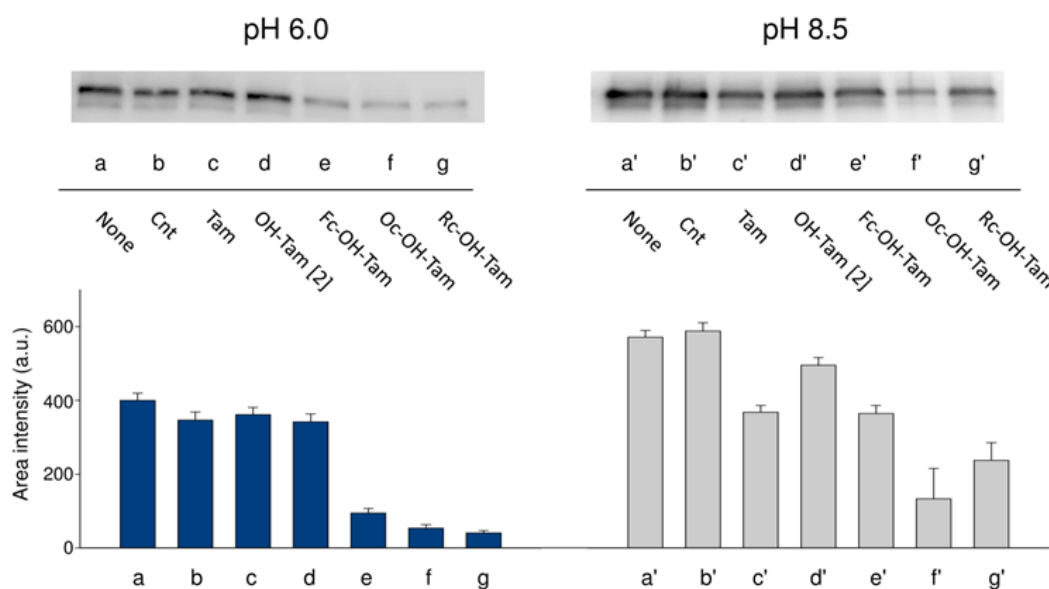
a) Compounds were incubated with TrxR1 or TrxR2 in the presence of NADPH. After 5 min, TrxR activity was estimated as described in Experimental section; b) Compounds were incubated in 0.2 M Tris-HCl buffer (pH 8.1) containing 1 mM EDTA, with 22 nM HRP and 0.1 mM H₂O₂ for 15 min at 25 °C. The mixture was then incubated with TrxR1 or TrxR2 as indicated in a); c) value from ref⁸; d) value from ref¹⁶

Both **Fc-OH-Tam** and **Oc-OH-Tam** were moderate inhibitors of both TrxR1 and TrxR2 with IC₅₀ between 15 and 23 μM, while **Rc-OH-Tam** was slightly active on TrxR1 and inactive on TrxR2. In contrast, none of the organic counterparts were active on both TrxR1 and TrxR2. Strikingly different results were obtained when the TLMs were enzymatically oxidized by a mixture of HRP and H₂O₂ for 15 min prior to incubation with TrxR. Indeed, all three TLMs became potent inhibitors of TrxR1 with a remarkably low IC₅₀ of 60 nM for the iron complex, followed by an IC₅₀ of 0.42 μM for the ruthenium complex and 1.2 μM for the osmium complex. It is also interesting to notice

that oxidized **Fc-OH-Tam** was significantly more active on TrxR1 than on TrxR2. Conversely, preliminary treatment of **OH-Tam[2]** and **OH-Tam[3]** by HRP/H₂O₂ led to moderate inhibition of only TrxR1 (IC₅₀ of ca. 8 μM) while HRP-treated Tam remained inactive on both TrxRs.

Metalloids interaction with the selenocysteine residue of TrxR

The C-terminal redox active site of TrxR is formed by a Cys-Sec motif (Sec = selenocysteine) which is the target of many electrophiles that inhibit TrxR by alkylation of Cys and/or Sec residues.

**Fig. 1.** BIAM assay **after treatment** of TrxR1 **treated with** compounds oxidized by HRP/H₂O₂

TLMs and Tam derivatives (2 μM) were treated with HRP/H₂O₂ for 15 min. The oxidized derivatives obtained (Ox-Mc with Mc = **Fc**, **Oc**, **Rc**; **Ox-OH-Tam[2]**, **Ox-Tam**) were incubated in the presence of a pre-reduced aliquot of TrxR1, as reported in Experimental section. Then, aliquots of the reaction mixture were added to 50 μM biotinylated iodoacetamide (BIAM) in either buffer at pH 6.0 (0.1 M Hepes-Tris) or pH 8.5 (0.1

M Tris-HCl) to alkylate the -SH/-SeH remaining groups. Proteins were transferred to a nitrocellulose membrane, and BIAM conjugated enzyme was detected with **streptavidin-horseradish peroxidase conjugate**. a, a': **None**; b, b': **Cnt**; c, c': **Ox-Tam**; d, d': **Ox-OH-Tam[2]**; e, e': **Ox-Fc**; f, f': **Ox-Oc**; g, g': **Ox-Rc**.

Discrimination between both residues can be achieved by carrying out the biotin-iodoacetamide (BIAM) assay. The pKa of both residues being different (pKa R-SeH/R-Se- = 5.24; pKa R-SH/R-S- = 8), selective alkylation by BIAM can be achieved according to the pH. At low pH (6), only the selenolate group of Sec is alkylated by BIAM while at high pH (8.5), both the thiolate and the selenolate groups of Cys and Sec are simultaneously alkylated by BIAM.³² Mixtures of TrxR1 and oxidized TLMs or organic tamoxifens were allowed to react with BIAM at pH 6 or 8.5 to alkylate the remaining selenolate and/or thiolate groups and the samples were submitted to Western blot analysis (Fig. 1). Very weak bands were observed for TrxR1 samples exposed to the oxidized TLMs then to BIAM at pH 6 while the organic analogues had no effect. In consequence, the three oxidized TLMs equally interacted with Sec by probable alkylation of the highly nucleophilic selenolate group. When alkylation by BIAM was carried out at pH 8.5, the TrxR1 sample exposed to **Oc-OH-Tam** gave a band weaker than the control, indicating that only oxidized **Oc-OH-Tam** was able to simultaneously alkylate thiol groups. In addition, the HRP/H₂O₂ mixture alone had no effect on the ability of BIAM to alkylate TrxR1 (**cnt**, lane b and b').

Activities of cytosolic and mitochondrial thioredoxin reductases in Jurkat cells

Jurkat cells (2×10^6) were incubated with each compound (15 μ M) for 18 h. Then the activity of total TrxR was determined in cell lysates (Fig. S2). A large decrease of total TrxR activity (60 to 95% inhibition) was observed in cells treated with the three TLMs while **Tam** and **OH-Tam[2]** induced a slight increase of activity and **OH-Tam[3]** had no effect. Additional experiments with **Fc-OH-Tam** showed that the activity of total TrxR was time-dependent as a slight increase was observed after 3 h followed by progressive and slow inhibition in the next 15 h (Fig. S3). After optimization of the ratio between compounds (30 μ M) and cell number (3×10^7), the activity of TrxR1 and TrxR2 was measured separately in the cytosolic and mitochondrial fractions of Jurkat cells (Fig. 2). High inhibition of TrxR2 was found for cells exposed to **Fc-OH-Tam** and **Rc-OH-Tam** (72% and 79.4% inhibition, respectively), while **Oc-OH-Tam** was less effective (44% inhibition). However, organic tamoxifens were significantly less potent (up to 27% inhibition). In contrast the effect of the three TLMs

on TrxR1 was less pronounced (25- 36 % inhibition) and not much different from that of the organic compounds (12-21 % inhibition).

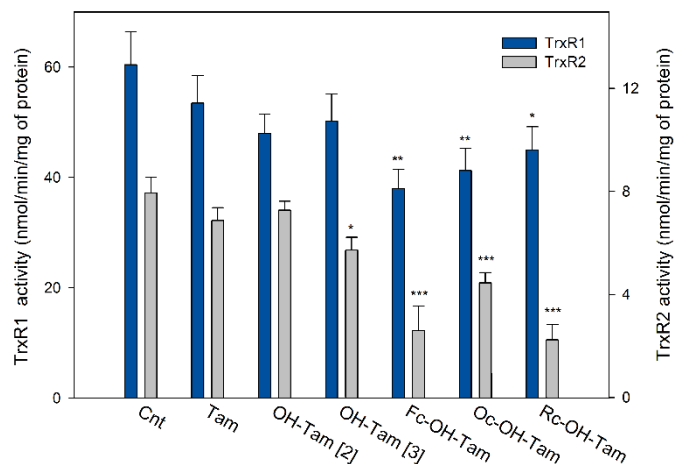


Fig. 2. TrxR1 and TrxR2 activities in Jurkat cells. Cytosolic and mitochondrial fractions were isolated from Jurkat cells treated with the different compounds (30 μ M/ 3×10^7 cells for 18 h), and TrxRs activities were estimated as reported in Experimental Section. *: $p < 0.05$; **: $p < 0.01$; ***: $p < 0.001$.

Mitochondrial thioredoxin (Trx2) redox state in Jurkat cells

As all three TLMs and not the organic analogues induced strong inhibition of TrxR2 in Jurkat cells, the redox state of Trx2 in cells exposed to each compound at 15 μ M for 18 h was evaluated by the protein electrophoretic mobility shift assay with iodoacetamide / iodoacetic acid (IAM/IAA) as follows.³³ Lysates of cells incubated with each compound were first treated with IAM to titrate free SH groups, then, after reaction with DTT to reduce disulphide bonds, IAA was added in order to derivatize the SH groups arising from previously oxidized cysteines. Samples were submitted to urea-PAGE in non-reducing conditions and the 3 states of Trx2 (fully oxidized, partially oxidized and fully reduced) were detected by Western blot analysis (Fig. 3).

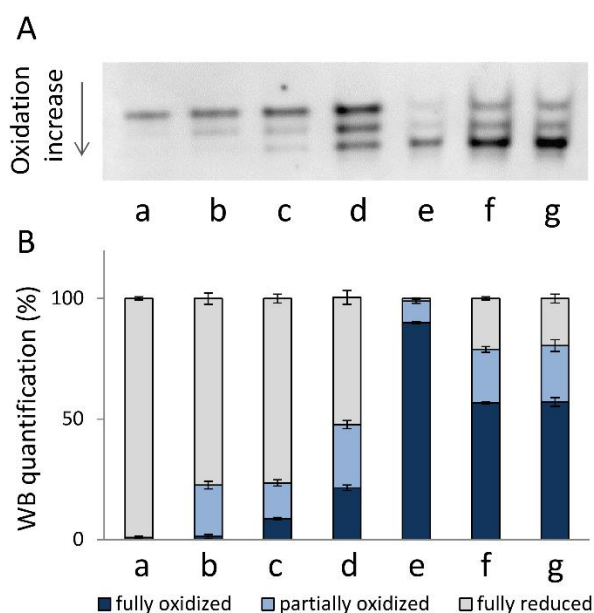


Fig. 3. Redox state of mitochondrial thioredoxin (Trx2) in Jurkat cells. Jurkat cells incubated for 18 h with 15 μM TLMs or organic tamoxifens were lysed and lysates treated with 10 mM IAM/IAA procedure to titrate reduced, partially oxidized and fully oxidized thiol groups. Redox state of Trx2 was then detected by Western Blot analysis (A). a: Cnt; b: Tam; c: OH-Tam[2]; d: OH-Tam[3]; e: Fc-OH-Tam; f: Oc-OH-Tam; g: Rc-OH-Tam. (B) Densitometric analysis of the lanes performed with ImageJ software.

Cells incubated with the 3 TLMs showed accumulation of the fully oxidized form of Trx2, especially those exposed to Fc-OH-Tam (90%) and to a lesser extent those exposed to the Rc-OH-Tam and Oc-OH-Tam (57%). Conversely, the fully reduced form of Trx2 was

predominant in cells exposed to Tam and OH-Tam[2] (77%). Only OH-Tam[3] induced the accumulation of a significant amount of oxidized forms of Trx2 (ca. 50%).

ROS production and evaluation of the mitochondrial membrane potential (MMP) in Jurkat cells

Short term (0-30 min) mitochondrial ROS production in Jurkat cells was first measured using the DHR dye, after cell incubation with 10 μM of TLMs or organic tamoxifens. We found that TLMs, but not the organic compounds increased the basal ROS production during this period (Fig. S4). Long term mitochondrial superoxide level was then evaluated in Jurkat cells incubated with 15 μM TLMs or organic tamoxifens after 18 h, by flow cytometry analysis using MitoSOX[™] Red as fluorescent probe (Fig. 4 left). A very high percentage of cells (72%) incubated with Fc-OH-Tam emitted high MitoSOX[™] fluorescence. This percentage was lower for cells incubated with Rc-OH-Tam and Oc-OH-Tam (around 40%) while the percentage of cells emitting high MitoSOX[™] fluorescence was insignificant for those incubated with the organic tamoxifens (6-8 %). The mitochondrial membrane potential (MMP) was evaluated on the same pool of cells by flow cytometry using the fluorescent dye TMRM (Fig. 4 right). The population of cells with low MMP was close to 100% for cells incubated with the three TLMs for 18 h while the three organic tamoxifens affected the MMP to a much lower extent (up to 37.5% for OH-Tam[3]). Interestingly, the rate of depolarization of the mitochondrial membrane was fast for Fc-OH-Tam since the percentage of cells displaying low MMP was already equal to 42% after 3 h (Fig. S5).

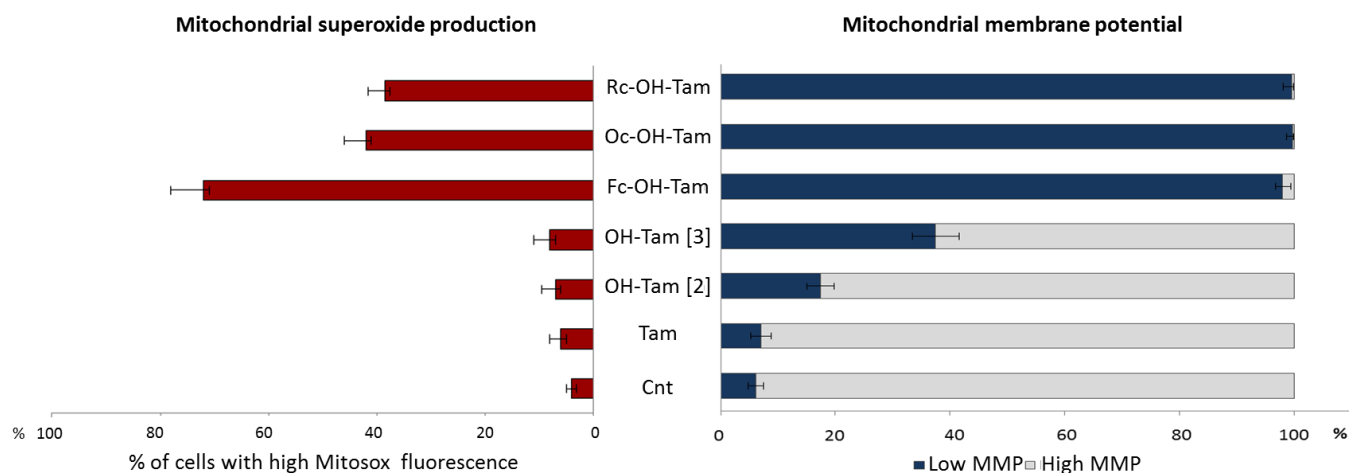


Fig. 4. Effects of TLMs and organic tamoxifens on mitochondrial superoxide production (left) and membrane potential (right) in Jurkat cells.

Cells were treated for 18 h with the various compounds (15 μ M). Then, aliquots of cells were incubated in PBS/10 mM glucose in the presence of 1 μ M MitoSOX for the determination of superoxide production, or 25 nM TMRM for the measurement of MMP. Fluorescence was detected using a flow cytometric analysis. The left panel reports quantification of superoxide production (red bars). The right panel shows the MMP analysis in Jurkat cells where dark blue corresponds to cell population with low membrane potential, while light gray is related to cell population with high membrane potential.

Activation of the apoptotic pathway

Release of cytochrome c and state of caspase 3 were examined in Jurkat cells exposed to the three TLMs or the organic tamoxifens for 18 h (Fig. 5).

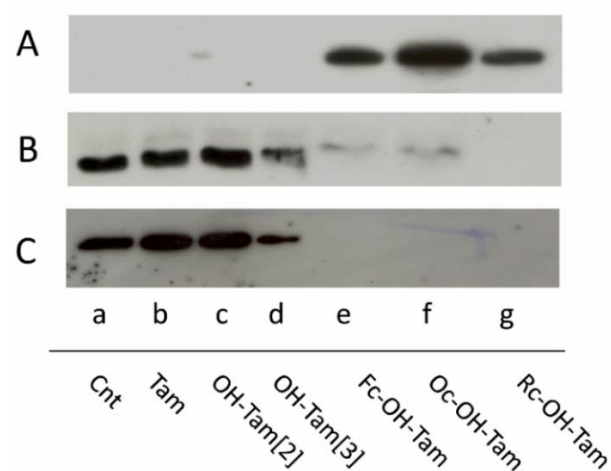


Fig. 5. Apoptosis pathway activation in Jurkat cells incubated with TLMs or tamoxifens derivatives. Jurkat cells (2×10^6) were treated for 18 h in the presence of 15 μ M compounds. Cytochrome c localization was evaluated in cytosol (A) and in mitochondria (B); pro-caspase-3 detection is reported in (C). a: Cnt; b: Tam; c: OH-Tam[2]; d: OH Tam[3]; e: Fc-OH-Tam; f: Oc-OH-Tam; g: Rc-OH-Tam

The results clearly show that after incubation with the three TLMs, cytochrome c was released from mitochondria to cytosol while it was still located in mitochondria for cells treated with organic tamoxifens. Moreover, pro-caspase 3 was only detected in cells exposed to organic tamoxifens and not in cells exposed to TLMs. Thus only TLMs and not organic tamoxifens were able to trigger cell apoptosis by the mitochondria-mediated pathway.

Intracellular distribution of metals in Jurkat cells

As we found that metalocifens induced mitochondria impairment we undertook, by ICP-OES, quantification of iron, ruthenium and osmium in mitochondria and cytosol of cells exposed to **Fc-OH-Tam**,

Rc-OH-Tam and **Oc-OH-Tam** (Table 3, Fig. S6). As iron is a metal present in cells its quantification was also performed in untreated cells.

Table 3. ICP-OES quantification of iron, ruthenium and osmium in cytosol and mitochondria of Jurkat cells incubated for 24h with 30 μ M **Fc-OH-Tam**, **Oc-OH-Tam** and **Rc-OH-Tam** and of iron in untreated cells

Compound	Cytosol (nmol/mg protein)	Mitochondria (nmol/mg protein)
Fc-OH-Tam ^{a)}	10 \pm 5	153 \pm 43
Oc-OH-Tam ^{b)}	5.5 \pm 4.9	108 \pm 31
Rc-OH-Tam ^{c)}	0.13 ^{d)}	75
Untreated cells (Fe)	1.5 \pm 0.9	19 \pm 11

a) mean of 3 experiments; b) mean of 2 experiments; c) single experiment; d) value in the range of the blanks.

The amounts of iron, osmium and ruthenium in the cytosol and in mitochondria were in the same order of magnitude, indicating that the three TLMs were all able to accumulate in cells with a high concentration in the mitochondria. The amount of iron in the cytosol and mitochondria of cells incubated with 30 μ M **Fc-OH-Tam** was significantly higher than the level of iron in control cells, indicating that it mostly originated from **Fc-OH-Tam** and not from the endogenous iron pool.

Subcellular distribution of the metals gave an almost exclusive localization in the nuclear crude fractions (45-54%) and mitochondria (37-50%) and only a marginal localization in the cytosol (5-9%) (Table 4).

Table 4. Subcellular distribution (%) of Fe and Os in Jurkat cells incubated with 30 μ M **Fc-OH-Tam** and **Oc-OH-Tam** for 24 h.

Compound	Cytosolic fraction (%)	Mitochondrial fraction (%)	Crude nuclear fraction (%)
Fc-OH-Tam ^{a)}	9 \pm 2	37 \pm 7	54 \pm 9
Oc-OH-Tam ^{b)}	5 \pm 2	50 \pm 7	45 \pm 4

a) mean of 3 experiments; b) mean of 2 experiments

Lipophilic cations are well known to preferentially localize in mitochondria.^{34,35} At physiological pH, the dimethylamino group of TLMs is protonated, thus they can be considered as lipophilic cations. Consequently, they are expected to target mitochondria. Such behaviour is also encountered for other lipophilic metal-based drug candidates of gold(I),³⁶ osmium(II),³⁷ and rhenium(I).³⁸

Discussion

In vitro inhibition of TrxR by TLMs occurred after their enzymatic oxidation by the HRP/H₂O₂ mixture and the products of oxidation were in general more active on the cytosolic isoform (IC₅₀ in the 0.06 - 1.2 μM range) than on the mitochondrial form (IC₅₀ in the 3.9 - 10.9 μM range, Table 1). On the contrary, oxidized organic tamoxifen derivatives were much poorer inhibitors of TrxR thus underlining the essential role played by the metallocenic entity in the oxidation profile and in the inactivation of TrxR. Independent spectroscopic studies showed that the species responsible for TrxR inhibition were their quinone methides for **Fc-OH-Tam** and **Rc-OH-Tam** and the quinone methide cation for **Oc-OH-Tam**, all display a highly electrophilic character. The inability of the HRP/H₂O₂ system to generate the QM of organic tamoxifens confirmed this assertion. Within the TLMs series, the extent of inhibition depends on both the metallocene unit and the TrxR isoform. Oxidized **Fc-OH-Tam** was significantly less efficient on TrxR2 than **Rc-OH-Tam** and **Oc-OH-Tam** while the reverse was observed for TrxR1 for which oxidized **Fc-OH-Tam** was the most active (IC₅₀ = 0.06 μM). This very low value is in the range of those measured for gold(I) complexes which are recognized as very potent inhibitors of TrxR.^{14,39-41}

The mechanism of inhibition of TrxR1 by the oxidized TLMs was investigated by the BIAM assay. This assay demonstrated that only the 3 oxidized TLMs and not the organic tamoxifens interacted with the C-terminal redox active site of TrxR1. Oxidized **Fc-OH-Tam** and **Rc-OH-Tam** selectively interacted with the penultimate selenocysteine residue while oxidized **Oc-OH-Tam** was also able to interact with the cysteine residues. The fact that the product of oxidation of **Oc-OH-Tam** is a quinone methide carbocation¹⁵ and not the neutral quinone methide may provide a rationale for this different reactivity.

A very different behaviour was observed in Jurkat cells, since the TLMs themselves were able to inhibit TrxR, indicating that their activation occurred *in cellulo* by endogenous oxidation systems.

Moreover, all three TLMs were more efficient inhibitors of TrxR2 compared to TrxR1. This rather puzzling result is easily understandable when considering the subcellular distribution of the complexes, namely low concentration in cytosol and high concentration in mitochondria. Such an inversion of selectivity was previously noticed for cationic and lipophilic gold(I) complexes that displayed the same ability to preferentially accumulate in mitochondria.⁴² The fact that inhibition of the mitochondrial thioredoxin system was coupled with alteration of the MMP, overproduction of ROS and translocation of cytochrome c may have to do with the recently reported deregulation of the redox state of cyclophilin D,³⁴ a mitochondrial enzyme involved in the regulation of the mitochondrial permeability transition process.⁴³ On the other hand, organic tamoxifens were far less potent TrxR inhibitors than metallocifens in cells. This finding is in line with the results on purified TrxR and highlights again the essential input of the metallocenic units on the biological activity of TLMs.

Among the three TLMs, **Fc-OH-Tam** behaved differently from the two other ones regarding the redox state of Trx2, as cells incubated with **Fc-OH-Tam** contained 90% of fully oxidized form of Trx2 but only 57% for **Rc-OH-Tam** and **Oc-OH-Tam**. **Fc-OH-Tam** also induced a higher level of mitochondrial superoxide and an early decrease of MMP. These differences may be accountable to the much lower redox potential of ferrocene derivatives (+0.4 V for Fc,⁷ versus +0.8 V for ruthenium,⁴⁴ and +0.6 V for Oc,¹⁵ in their analogous metallociphenols). Indeed, according to Kovacic, only the metallocenes with a redox potential between +0.4 and -0.44 V display anticancer activity since this range of potentials is favorable for *in vivo* electron transfer and redox cycling.⁴⁵ In our series, only **Fc-OH-Tam** fulfils this requirement.

Conclusion

We showed that TLMs became strong inhibitors of both isoforms of TrxR after their enzymatic oxidation with HRP/H₂O₂. All the oxidized TLMs were stronger inhibitors of the cytosolic isoform TrxR1 with **Fc-OH-Tam** showing a remarkably low IC₅₀ of 60 nM. In Jurkat cells, TLMs preferentially accumulated in mitochondria as compared to cytosol. Accordingly, they preferentially inhibited the mitochondrial isoform of TrxR and stimulated the oxidation of Trx2, leading to cell redox imbalance.

The induced permeability of the mitochondrial membrane elicited release of cytochrome c and activation of the caspase pathway leading to cell apoptosis. This type of death found in Jurkat cells differs from that previously found in adherent tumour cells MDA-MB-231 where senescence was mainly observed. This study uncovers for the first time the powerful pro-apoptotic effects of TLMs that appear to be responsible for their cytotoxicity in a lymphoblastoid cancer cell line and could be relevant for future clinical applications in the chemotherapy of resistant tumours.

Abbreviations

BIAM	biotin iodoacetamide
DHR	dihydrorhodamine 123
Fc-OH-Tam	1-[4-[3-(Dimethylamino)propyloxy]phenyl]1-(4-hydroxyphenyl)-2-ferrocenyl-1-butene;
HRP	horseradish peroxidase;
ICP-OES	Inductively Coupled Plasma Optical Emission Spectroscopy;
MMP	mitochondrial membrane potential;
Oc-OH-Tam	1-[4-[3-(Dimethylamino)propyloxy]phenyl]1-(4-hydroxyphenyl)-2-osmocenyl-1-butene;
Rc-OH-Tam	1-[4-[3-(Dimethylamino)propyloxy] phenyl]-1-(4-hydroxyphenyl)-2-ruthenocenyl-1-butene;
Tam	tamoxifen, [1-[4-[2-(Methylamino)ethoxy]phenyl]-1,2-diphenyl-1-buten-1-yl]yl;
OH-Tam[2]	4-hydroxy-tamoxifen,(E/Z)-4-[1-[4-[2-(Methylamino)ethoxy]phenyl]-2-phenyl-1-buten-1-yl]-phenol;
OH-Tam[3]	(E/Z)-4-[1-[4-[2-(Methylamino)propyl]phenyl]-2-phenyl-1-buten-1-yl]-phenol;
RFU	relative fluorescence unit;
TLMs	tamoxifen-like metalocifens,
TMRM	tetramethyl rhodamine methyl ester
TNBC	triple negative breast cancer;
TrxR	thioredoxin reductase
TrxR1	cytosolic thioredoxin reductase
TrxR2	mitochondrial thioredoxin reductase
Trx	thioredoxin

Acknowledgements

Authors acknowledge COST Actions CM1105 and CM1106 for financial support and for allowing fruitful collaboration, Dr Benoit Caron and Dr Benoit Villemant in charge of ALIPP6 platform at University Pierre et Marie Curie Paris for assistance in the ICP-OES experiments.

References

1. N. Harbeck and M. Gnant, Breast Cancer, *Lancet*, 2017, **389**, 1134-1150.
2. G. Jaouen, A. Vessieres and S. Top, Ferrocifen type anti cancer drugs, *Chem. Soc. Rev.*, 2015, **44**, 8802-8817.
3. S. Top, A. Vessières, G. Leclercq, J. Quivy, J. Tang, J. Vaissermann, M. Huché and G. Jaouen, Synthesis, biochemical properties and molecular modelling studies of organometallic specific estrogen receptor modulators (SERMs), the ferrocifens and hydroxyferrocifens: evidence for an antiproliferative effect of hydroxyferrocifens on both hormone-dependent and hormone-independent breast cancer cell lines, *Chem. Eur. J.*, 2003, **9**, 5223-5236.
4. A. L. Laine, E. Adriaenssens, A. Vessières, G. Jaouen, C. Corbet, E. Desruelles, P. Pigeon, R. A. Toillon and C. Passirani, The in vivo performance of ferrocenyl tamoxifen lipid nanocapsules in xenografted triple negative breast cancer, *Biomaterials*, 2013, **34**, 6949-6956.
5. Q. Michard, G. Jaouen, A. Vessières and B. A. Bernard, Evaluation of the cytotoxic properties of organometallic ferrocifens on melanocytes, primary and metastatic melanoma cells, *J. Inorg. Biochem.*, 2008, **102**, 1980-1985.
6. A. Vessières, C. Corbet, J. M. Heldt, N. Lories, N. Jouy, I. Laios, G. Leclercq, G. Jaouen and R. A. Toillon, A ferrocenyl derivative of hydroxytamoxifen elicits an estrogen receptor-independent mechanism of action in breast cancer cell lines, *J. Inorg. Biochem.*, 2010, **104**, 503-511.
7. E. A. Hillard, A. Vessières, L. Thouin, G. Jaouen and C. Amatore, Ferrocene-mediated proton-coupled electron transfer in a series of ferrocifen-type breast cancer drug candidates., *Angew. Chem. Int. Ed.*, 2006, **45**, 285-290.
8. A. Citta, A. Folda, A. Bindoli, P. Pascal Pigeon, S. Top, A. Vessières, M. Salmain, G. Jaouen and M. P. Rigobello, Evidence for targeting thioredoxin reductases with ferrocenyl quinone methides. A possible molecular basis for the antiproliferative effect of hydroxyferrocifens on cancer cells, *J. Med. Chem.*, 2014, **57**, 8849-8859.
9. W. Q. Cai, L. W. Zhang, Y. L. Song, B. L. Wang, B. X. Zhang, X. M. Cui, G. M. Hu, Y. P. Liu, J. C. Wu and J. G. Fang, Small molecule inhibitors of mammalian thioredoxin reductase, *Free Radic. Biol. Med.*, 2012, **52**, 257-265.
10. V. Gandin and A. P. Fernandes, Metal- and Semimetal-Containing Inhibitors of Thioredoxin Reductase as Anticancer Agents, *Molecules*, 2015, **20**, 12732-12756.
11. Y. Liu, Y. J. Li, S. H. Yu and G. S. Zhao, Recent Advances in the Development of Thioredoxin Reductase Inhibitors as Anticancer Agents, *Curr. Drug Targets*, 2012, **13**, 1432-1444.
12. F. Saccoccia, F. Angelucci, G. Boumis, D. Carotti, G. Desiato, A. E. Miele and A. Bellelli, Thioredoxin Reductase and its Inhibitors, *Curr. Protein Pept. Sci.*, 2014, **15**, 621-646.
13. A. Bindoli and M. P. Rigobello, Principles in Redox Signaling: From Chemistry to Functional Significance, *Antioxid. Redox Sign.*, 2013, **18**, 1557-1593.
14. A. Bindoli, M. P. Rigobello, G. Scutari, C. Gabbiani, A. Casini and L. Messori, Thioredoxin reductase: A target for gold compounds acting as potential anticancer drugs, *Coord. Chem. Rev.*, 2009, **253**, 1692-1707.

15. H. Z. S. Lee, O. Buriez, F. Chau, E. Labbé, R. Ganguly, C. Amatore, G. Jaouen, A. Vessières, W. K. Leong and S. Top, Synthesis, characterization, and biological properties of osmium-based tamoxifen derivatives. Comparison with their homologues in the iron and ruthenium series, *Eur. J. Inorg. Chem.*, 2015, 4217–4225.
16. V. Scalcon, S. Top, H. Z. S. Lee, A. Citta, A. Folda, A. Bindoli, W. K. Leong, M. Salmain, A. Vessieres, G. Jaouen and M. P. Rigobello, Osmocenyl-tamoxifen derivatives target the thioredoxin system leading to a redox imbalance in Jurkat cells, *J. Inorg. Biochem.*, 2016, **160**, 296–304.
17. M. Luthman and A. Holmgren, Rat-liver thioredoxin and thioredoxin reductase - purification and characterizaion *Biochemistry*, 1982, **21**, 6628–6633.
18. M. P. Rigobello and A. Bindoli, in *Methods in Enzymology, Vol 474: Thiol Redox Transitions in Cell Signaling, Pt B: Cellular Localization and Signaling*, eds. E. Cadenas and L. Packer, 2010, vol. 474, pp. 109–122.
19. O. H. Lowry, N. J. Rosebrough, A. L. Farr and R. J. Randall, Protein measurement with the folin phenol reagent *J. Biol. Chem.*, 1951, **193**, 265–275.
20. J. G. Fang, J. Lu and A. Holmgren, Thioredoxin reductase is irreversibly modified by curcumin - A novel molecular mechanism for its anticancer activity, *J. Biol. Chem.*, 2005, **280**, 25284–25290.
21. S. Prast-Nielsen, M. Cebula, I. Pader and E. S. J. Arner, Noble metal targeting of thioredoxin reductase - covalent complexes with thioredoxin and thioredoxin-related protein of 14 kDa triggered by cisplatin, *Free Radic. Biol. Med.*, 2010, **49**, 1765–1778.
22. D. A. Clayton and G. S. Shadel, Isolation of mitochondria from cells and tissues, *Cold Spring Harbor Protoc.* (10), 2014, **pdb top074542**.
23. N. A. Bersani, J. R. Merwin, N. I. Lopez, G. D. Pearson and G. F. Merrill, Protein electrophoretic mobility shift assay to monitor redox state of thioredoxin in cells, *Methods Enzymol.*, 2002, **347**, 317–326.
24. J. Ungerstedt, Y. Du, H. Zhang, D. Nair and A. Holmgren, In vivo redox state of Human thioredoxin and redox shift by the histone deacetylase inhibitor suberoylanilide hydroxamic acid (SAHA), *Free Radic. Biol. Med.*, 2012, **53**, 2002–2007.
25. P. Pigeon, S. Top, A. Vessières, M. Huché, E. A. Hillard, E. Salomon and G. Jaouen, Selective estrogen receptor modulators (SERMs) in the Ruthenocene series. Synthesis and biological behavior, *J. Med. Chem.*, 2005, **48**, 2814–2821.
26. S. Top, I. Efremenko, M. N. Rager, A. Vessieres, P. Yaswen, G. Jaouen and R. H. Fish, Derivatives Reacting with Cp*Rh Complexes that involve eta(1)-N, eta(2)-N,O, eta(1)-O, and eta(6) Bonding Modes, *Inorg. Chem.*, 2011, **50**, 271–284.
27. P. Messina, E. Labbé, O. Buriez, E. A. Hillard, A. Vessières, D. Hamels, S. Top, G. Jaouen, Y. M. Frapart, D. Mansuy and C. Amatore, Deciphering the activation sequence of ferrociphenol anticancer drug candidates, *Chem. Eur. J.*, 2012, **18**, 6581–6587.
28. P. W. Fan, F. Zhang and J. L. Bolton, 4-hydroxylated metabolites of the antiestrogens tamoxifen and toremifene are metabolized to unusually stable quinone methides., *Chem. Res. Toxicol.*, 2000, **13**, 45–52.
29. A. M. Davies, M. E. Malone, E. A. Martin, R. M. Jones, R. Jukes, C. K. Lim, L. L. Smith and I. N. H. White, Peroxidase activation of 4-hydroxytamoxifen to free radicals detected by EPR spectroscopy, *Free Radic. Biol. Med.*, 1997, **22**, 423–431.
30. M. I. Rybinskaya, A. Z. Kreindlin and S. S. Fadeeva, On the problem of stabilization of alpha-carbocationic centers in metallocene series – related interconversions of permethylated alpha-metallocenyl carbocations and metallocenium cation-radicals of the iron sub-group, *J. Organomet. Chem.*, 1988, **358**, 363–374.
31. M. I. Rybinskaya, A. Z. Kreindlin, Y. T. Struchkov and A. I. Yanovsky, On the problem of stabilization of alpha-metallocenyl carbocation – synthesis, properties and Crystal-structure of C5ME5OSC5ME4CH2+ BPH4-CH2CL2, *J. Organomet. Chem.*, 1989, **359**, 233–243.
32. J. R. Kim, H. W. Yoon, K. S. Kwon, S. R. Lee and S. G. Rhee, Identification of proteins containing cysteine residues that are sensitive to oxidation by hydrogen peroxide at neutral pH, *Anal. Biochem.*, 2000, **283**, 214–221.
33. Y. T. Du, H. H. Zhang, X. Zhang, J. Lu and A. Holmgren, Thioredoxin 1 Is Inactivated Due to Oxidation Induced by Peroxiredoxin under Oxidative Stress and Reactivated by the Glutaredoxin System, *J. Biol. Chem.*, 2013, **288**, 32241–32247.
34. A. Folda, A. Citta, V. Scalcon, T. Cali, F. Zonta, G. Scutari, A. Bindoli and M. P. Rigobello, Mitochondrial Thioredoxin System as a Modulator of Cyclophilin D Redox State, *Sci. Rep.*, 2016, **6**, 23071 ; doi:23010.21038/srep23071.
35. M. C. Frantz and P. Wipf, Mitochondria as a Target in Treatment, *Environ. Mol. Mutagen.*, 2010, **51**, 462–475.
36. L. Oehninger, R. Rubbiani and I. Ott, N-Heterocyclic carbene metal complexes in medicinal chemistry, *Dalton Trans.*, 2013, **42**, 3269–3284.
37. S. H. van Rijjt, I. Romero-Canelon, Y. Fu, S. D. Shnyder and P. J. Sadler, Potent organometallic osmium compounds induce mitochondria-mediated apoptosis and S-phase cell cycle arrest in A549 non-small cell lung cancer cells, *Metallomics*, 2014, **6**, 1014–1022.
38. S. Imstepf, V. Pierroz, R. Rubbiani, M. Felber, T. Fox, G. Gasser and R. Alberto, Organometallic Rhenium Complexes Divert Doxorubicin to the Mitochondria, *Angew. Chem. Int. Ed.*, 2016, **55**, 2792–2795.
39. A. Citta, E. Schuh, F. Mohr, A. Folda, M. L. Massimino, A. Bindoli, A. Casini and M. P. Rigobello, Fluorescent silver(I) and gold(I)-N-heterocyclic carbene complexes with cytotoxic properties: mechanistic insights, *Metallomics*, 2013, **5**, 1006–1015.
40. O. Rackham, S. J. Nichols, P. J. Leedman, S. J. Berners-Price and A. Filipovska, A gold(I) phosphine complex selectively induces apoptosis in breast cancer cells: Implications for anticancer therapeutics targeted to mitochondria, *Biochem. Pharmacol.*, 2007, **74**, 992–1002.
41. E. Schuh, C. Pfluger, A. Citta, A. Folda, M. P. Rigobello, A. Bindoli, A. Casini and F. Mohr, Gold(I) Carbene Complexes Causing

- Thioredoxin 1 and Thioredoxin 2 Oxidation as Potential Anticancer Agents, *J. Med. Chem.*, 2012, **55**, 5518-5528.
42. O. Rackham, A. M. J. Shearwood, R. Thyer, E. McNamara, S. M. K. Davies, B. A. Callus, A. Miranda-Vizuete, S. J. Berners-Price, Q. Cheng, E. S. J. Arner and A. Filipovska, Substrate and inhibitor specificities differ between human cytosolic and mitochondrial thioredoxin reductases: Implications for development of specific inhibitors, *Free Radic. Biol. Med.*, 2011, **50**, 689-699.
43. A. P. Halestrap and A. P. Richardson, The mitochondrial permeability transition: A current perspective on its identity and role in ischaemia/reperfusion injury, *J. Mol. Cell. Cardiol.*, 2015, **78**, 129-141.
44. H. Z. S. Lee, O. Buriez, E. Labbé, S. Top, P. Pigeon, G. Jaouen, C. Amatore and W. K. Leong, Oxidative Sequence of a Ruthenocene-Based Anticancer Drug Candidate in a Basic Environment, *Organometallics*, 2014, **33**, 4940-4946.
45. P. Kovacic, Unifying mechanism for anticancer agents involving electron transfer and oxidative stress: Clinical implications, *Medical Hypotheses*, 2007, **69**, 510-516.